IET Microwaves, Antennas & Propagation

Research Article

IET Journals
The Institution of Engineering and Technology

Simulation and design of a tuneable ferrite resonator antenna based on nanostructured nickel ferrite material

ISSN 1751-8725
Received on 22nd April 2014
Revised on 10th June 2015
Accepted on 26th June 2015
doi: 10.1049/iet-map.2014.0663
www.ietdl.org

V.P. Silva Neto[1] ✉, *C.F.L. Vasconcelos*[1], *M.R.D. Bomio*[2], *M.R.M.L. Albuquerque*[1], *J.H. Araújo*[3], *A.G. D'Assunção*[1]

[1]*Departamento de Engenharia de Comunicações, Universidade Federal do Rio Grande do Norte (UFRN), 59078-970 Natal, RN, Brazil*
[2]*LSQM – Laboratório de Síntese Química de Materiais, Universidade Federal do Rio Grande do Norte (UFRN), 59078-970 Natal, RN, Brazil*
[3]*Departamento de Física Teórica e Experimental, Universidade Federal do Rio Grande do Norte (UFRN), 59078-970 Natal, RN, Brazil*
✉ *E-mail: valdemir.neto@yahoo.com.br*

Abstract: A tuneable ferrite resonator antenna (FRA) based on nanostructured nickel ferrite ($NiFe_2O_4$) material is proposed. Magnetic and dielectric characteristics are determined for the $NiFe_2O_4$ material such as electrical permittivity, and hysteresis loops. This ferrite material is used as a microwave resonator in the designing and fabrication of a cylindrical FRA. Ansoft high-frequency structure simulator software is used to provide simulated results for the antenna parameters such as resonant frequency, return loss, input impedance, and radiation pattern. A resonant frequency tuning capability with the application of a varied external magnetic bias field is shown. Measurement of the antenna prototype is also carried out and the obtained results are in good agreement with the simulated ones.

1 Introduction

Magnetic materials have been widely used for high frequency applications such as telecommunications and radar systems. The development of new devices and the increased level of integration of these devices into various applications have stimulated the development of magnetic materials with desired characteristics.

Ferrites constitute an important class of magnetic materials and are employed in a broad range of applications. Several features, such as ease of preparation, remarkable flexibility in tailoring the magnetic properties, and performance considerations make ferrites one of the most promising materials for microwave applications. In particular, ferrites have been used extensively due to their high permittivity and good loss characteristics at high frequencies. Among various ferrites, nanostructured nickel ferrite ($NiFe_2O_4$) has received special attention due to its novel and intriguing properties for widespread technological applications [1].

$NiFe_2O_4$ is regarded as a soft magnetic ferrite material with a completely inverse spinel structure, high resistivity, high magnetic permeability, and low eddy current losses, which make it suitable for high frequency applications. These features have opened new perspectives for technological applications, such as electromagnetic wave absorbers [2], gas sensors [3], lithium ion batteries [4, 5], and telecommunication applications [6].

Recently, the synthesis of $NiFe_2O_4$ by wet chemical synthesis has produced nanoparticles with good homogeneity, high sinterability, and good control of stoichiometry [7]. The Pechini method has been used as strategic synthesis route, because of its potential advantages such as low processing time, low energy consumption, and the possibility to produce $NiFe_2O_4$ into nanoscale, allowing the observation of new material properties that were not detected in microscale.

Dielectric resonator antennas (DRA) [8–10] and ferrite resonator antennas (FRA) [11–13] are experiencing increased use in antenna applications due to their interesting characteristics, such as the low weight, compact size, reduced fabrication cost, high radiation efficiency, improved bandwidth, and ability to integrate with other active and passive microwave components. Another advantage of these antennas is their inherently low loss due to the absence of conductors and surface wave losses. In contrast, at microwave frequencies, the conductor losses on conventional microstrip antennas may become significant due to the skin effect.

Generally, dielectric materials with high relative permittivity have been used in the development of DRA. Most microwave ferrites have high relative permittivity, hence they can be used in place of dielectric materials. When the ferrite is unbiased, its permeability is scalar and the FRA behaves as a DRA [12]. Though several geometries have been investigated, the cylindrical FRA is the most common structure taking into account the simplicity in the analysis, design, and fabrication [11].

Furthermore, the reason for the growing interest in FRA is mainly due to the fact that these devices can be tailored by changing the external static magnetic bias field, and thus, resonant frequency can be tuned. This benefit means flexibility and versatility over a wide frequency range, allowing designers to suit many requirements [12, 14].

In this paper, the use of nickel ferrite ($NiFe_2O_4$) material in the design of FRA is under consideration. Ferrite synthesis and the study of the electric and magnetic characteristics of the composites are carried out by means of experimental manipulation. Frequency response and radiation behaviour of the FRA are performed using the Ansoft high-frequency structure simulator (HFSS), a software package based on the finite-element method. Experimental results for the unbiased FRA based on nickel ferrite ($NiFe_2O_4$), processed at 900°C, are performed. The ferrite antenna is fed through a 50 Ω microstrip line.

2 $NiFe_2O_4$ material synthesis and characterisation

The $NiFe_2O_4$ nanoparticles were synthesised by the polymeric precursor method. Stoichiometric amounts of nickel nitrate ($Ni(NO_3)_2.6H_2O$) and ferric nitrate ($Fe(NO_3)_3.9H_2O$) were used. Iron citrate was formed by dissolution of ferric nitrate in an aqueous solution of citric acid (60–70°C). After homogenisation of the iron solution, ($Ni(NO_3)_2.6H_2O$) was slowly added and after complete dissolution of the nickel nitrate, salt and ethylene glycol were added to promote polymerisation of the mixed citrates by polyesterification reaction. The molar ratio between the iron and nickel cations was 1:1, the citric acid/metal ratio was fixed at 3:1, and the citric acid/ethylene glycol ratio was fixed at 60/40 (mass ratio). The resulting transparent brown colour solution was evaporated at 120°C under constant stirring condition, and

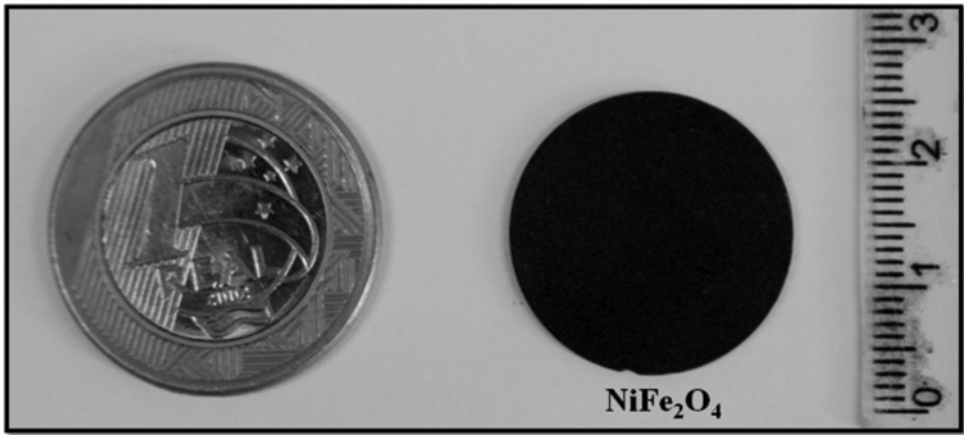

Fig. 1 *Photograph of the antenna prototype based on a nanostructured ($NiFe_2O_4$) ferrite material 193 × 87 mm (300 × 300 DPI)*

continuous evaporation leads to the gel formation. Resulting black colour gel was heated at 350°C for 2 hours with a heating rate of 10°C/min for pyrolysis of the organic material. The obtained $NiFe_2O_4$ powders were pressed into tablets of 7.26 mm diameter and 0.963 mm thickness, under 15 MPa pressure. Then, the compacted tablets were heat processing in a furnace at 900°C for 12 hours with a heating rate of 5°C/min in the air atmosphere.

The structural characterisation was performed by X-ray diffraction (XRD) using a Shimadzu X-ray diffractometer XRD 7000, with Cu Kα radiation ($\lambda = 1.5418$ Å) operating with copper target tube at a voltage of 40 kV and 30 mA of current in the 2θ range from 10° to 75°, and step size of 0.02°/min.

The morphologies were investigated using field-emission gun scanning electron microscopy (FEG-SEM, Carl Zeiss, model Supra 35-VP, Germany) operated at 6 kV. The magnetic properties of the sample were measured using a vibrant sample magnetometer (VSM). The sample used in the magnetic measurement was a piece with a mass of 0.0185 g taken from the sintered cylinder used in the antenna. The prototype of the ferrite material performed in this work is shown in Fig. 1.

3 FRA structure

The geometry of the proposed nanostructured FRA is depicted in Fig. 2. It consists of a ferrite disk of high permittivity mounted on top of a grounded dielectric substrate of low permittivity. The unbiased ferrite disk has radius a, height h, relative permeability μ_{r1}, and relative permittivity ε_{r1}.

The fabricated FRA is placed on FR4 dielectric substrate with scalar permittivity $\varepsilon_r = 4.4$, loss tangent $\tan\delta = 0.02$, and thickness $d = 1.57$ mm. The overall dielectric substrate dimensions are length $L = 10$ cm and width $W = 5$ cm. The antenna is fed by a 50 Ω microstrip line printed on the same substrate. The microstrip line feeding length is chosen to be $L_m = \lambda_0/4 = 13$ mm, where λ_0 is the guided wavelength corresponding to the centre operation frequency, $f_0 = 3.5$ GHz, of the unbiased FRA.

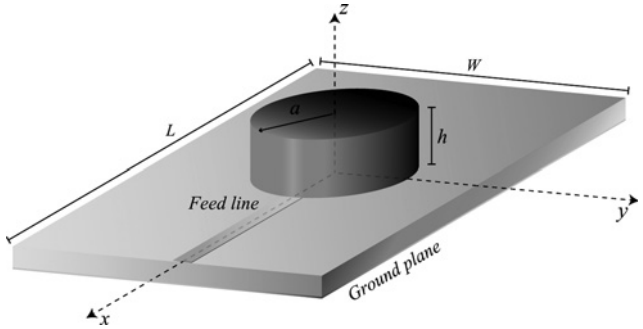

Fig. 2 *Geometry of the cylindrical FRA 96 × 51 mm (300 × 300 DPI)*

The physical parameters of the unbiased ferrite resonator used in the antenna design are summarised in Table 1.

When the structure is magnetised by an external dc magnetic field, H_0, applied perpendicularly to the ferrite (z-direction), the magnetic permeability tensor is given by [15]

$$\vec{\mu} = \begin{bmatrix} \mu & jk & 0 \\ -jk & \mu & 0 \\ 0 & 0 & \mu_0 \end{bmatrix} \tag{1}$$

with the components μ and k being expressed as

$$\frac{\mu}{\mu_0} = 1 - \frac{\gamma^2 H_0 4\pi M_s}{\omega^2 - (\gamma H_0)^2} \tag{2}$$

$$\frac{k}{\mu_0} = \frac{\gamma 4\pi M_s}{\omega^2 - (\gamma H_0)^2} \tag{3}$$

where ω is the operating frequency, γ is the gyromagnetic ratio, H_0 is the applied biasing field, $4\pi M_s$ is the saturation magnetisation of the ferrite, and μ_0 is the free-space permeability.

4 Results and discussion

Fig. 3 shows the X-ray patterns of $NiFe_2O_4$ powder processed at 900°C for 12 hours. XRD patterns revealed that all diffraction peaks of $NiFe_2O_4$ nanoparticles can be indexed to the cubic structure without the presence of α-Fe_2O_3 or NiO secondary phases, in agreement with the respective Joint Committee on Powder Diffraction Standards (JCPDS), card no. 89–4927. Moreover, the relative intensities and sharp diffraction of all peaks indicated that the materials are well-crystallised, suggesting an ordered structure at long range. Inset in Fig. 3, FEG-SEM image shows that the $NiFe_2O_4$ nanoparticles prepared by polymeric precursor method at 900°C, for 12 hours, present uniform, almost spherical morphology, with agglomeration of nanoparticles. The average particle size was determined from the FEG-SEM

Table 1 Parameters of the fabricated cylindrical ferrite resonator for the unbiased case

Parameter	Ferrite processed at 800°C	Ferrite processed at 900°C
a	7.26 mm	7.26 mm
h	0.963 mm	0.963 mm
ε_{r1}	9.20	13.135
μ_{r1}	1	1

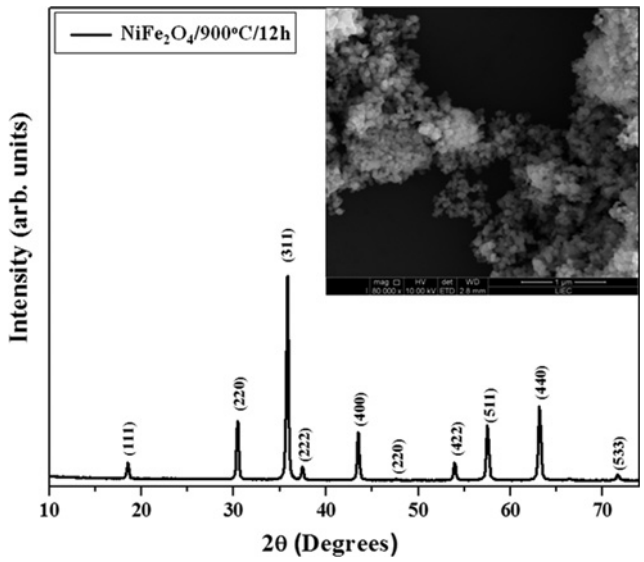

Fig. 3 *XRD patterns of the $NiFe_2O_4$ powder processed at 900°C for 12 h. Inset, FEG-SEM micrograph of spherical $NiFe_2O_4$ nanoparticles 184 × 157 mm (96 × 96 DPI)*

micrographs, which exhibited a particle distribution in the range of 45 nm.

Magnetic measurements of the $NiFe_2O_4$ sample were performed using a VSM. The sample with a mass of 0.0185 g was taken from the sintered cylinder used in the antenna prototype. Fig. 4 shows the magnetic hysteresis loop of the sample processed at 900°C for 12 hours. The saturation magnetisation (M_s) is 23.5 emu/g and the coercive field (H_c) is 13 Oe, which can be attributed as typical values of a soft magnetic material.

Fig. 5 depicts the influence of the applied dc magnetic bias field on the return loss of the FRA as function of frequency. The ferrite (900°C) has relative dielectric permittivity $\varepsilon_r = 13.13$, saturation magnetisation $4\pi M_s = 5240$ G, and gyromagnetic ratio $\gamma = 2.855$ MHz/Oe. Numerical simulations are carried out with the bias field applied perpendicularly to the ground plane. The curves for the input reflection coefficient S_{11} are obtained for different values of the magnetic bias field H_0. Return losses for the antenna are −23.84 dB at 3.605 GHz, −24.94 dB at 3.758 GHz, −14.58 dB at 4.065 GHz, and −12.67 dB at 4.310 GHz, with bias field H_0 equal to 0, 1000, 2500, and 3000 Oe, respectively. Observe the effect of

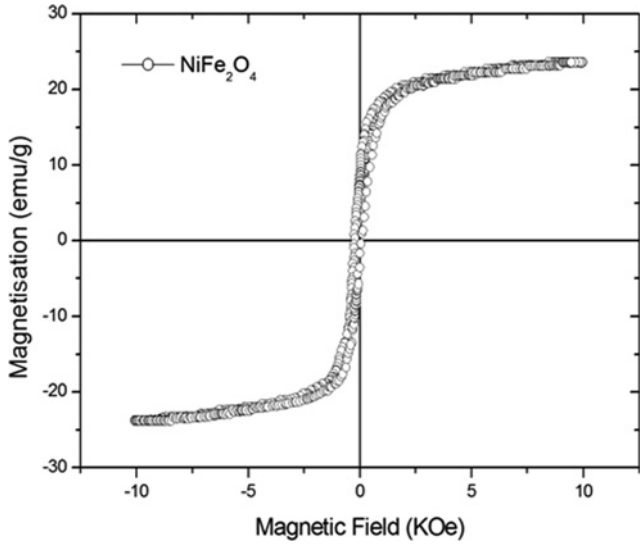

Fig. 4 *Magnetic hysteresis of the $NiFe_2O_4$ 126 × 107 mm (96 × 96 DPI)*

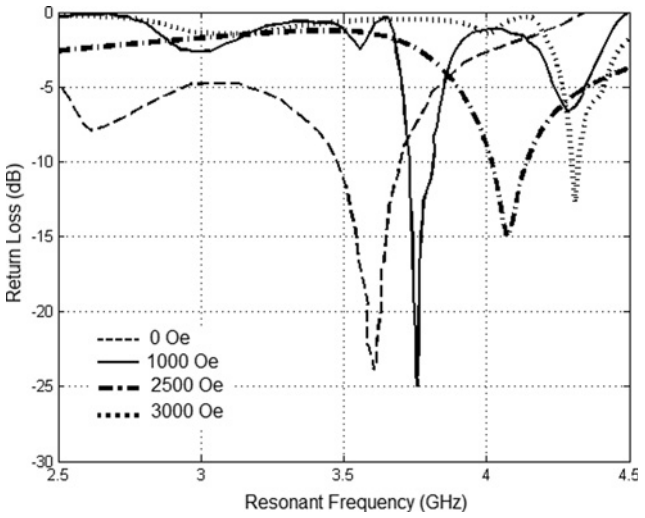

Fig. 5 *Simulated return loss for different values of the magnetic-bias field 145 × 116 mm (96 × 96 DPI)*

a varying bias on the resonant frequency and a magnetic tuning possibility, as shown in Table 2.

Fig. 6 shows simulated results for the resonant frequency of the proposed antenna versus the magnitude of the applied dc magnetic bias field H_0. The results are obtained for FRA using $NiFe_2O_4$ processed at 800°C and 900°C, respectively. The bias field is applied perpendicularly to the ground plane. It is noted that the resonant frequency of the antenna shifts to a higher frequency as the applied magnetic field strength increases and that the processing temperature of the ferrite material influences the operation frequency of the FRA.

Fig. 7 shows the simulated return loss versus frequency for the FRA using $NiFe_2O_4$ ferrite processed at 800°C and 900°C for 12

Table 2 Frequency response of FRA polarised with different dc magnetic fields

H_0, Oe	Resonant frequency, GHz	Return loss, dB	Bandwidth, MHz
0	3.605	−23.84	223
1000	3.758	−24.94	82
2500	4.065	−14.58	128
3000	4.310	−12.65	28

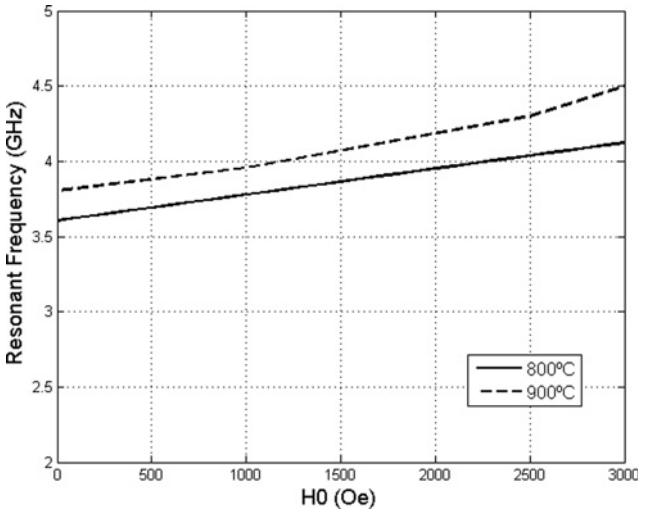

Fig. 6 *Simulated resonant frequency versus applied magnetic bias field 174 × 131 mm (96 × 96 DPI)*

IET Microw. Antennas Propag., 2015, Vol. 9, Iss. 14, pp. 1618–1622

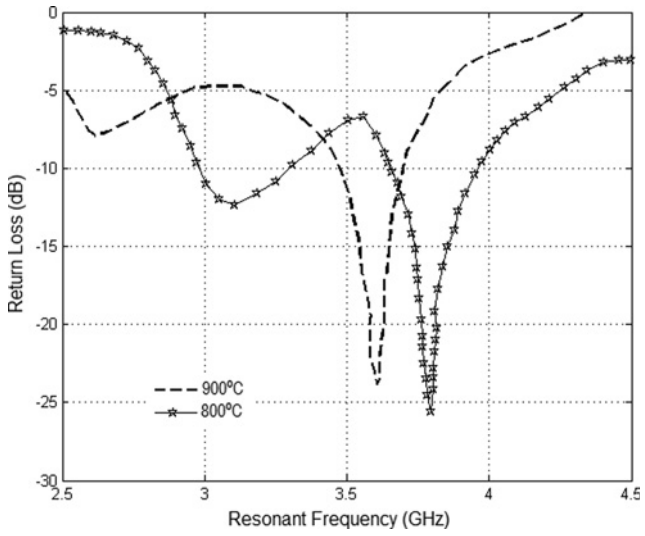

Fig. 7 *Simulated results for insertion loss of FRA antenna 144 × 119 mm (96 × 96 DPI)*

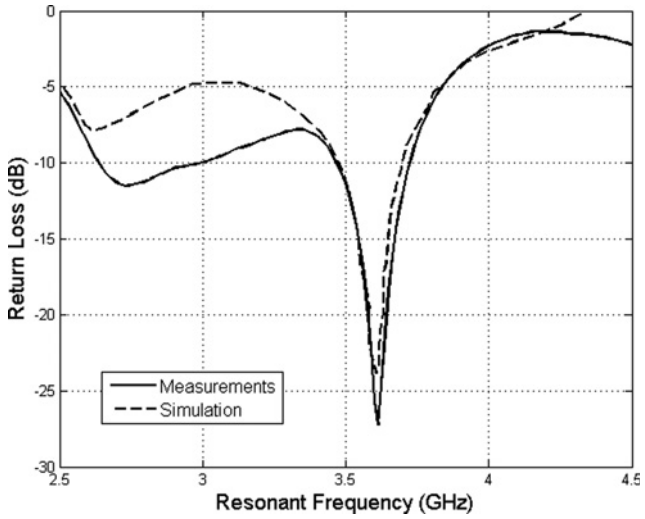

Fig. 8 *Simulated and measured results for return loss of FRA processed at 900°C 174 × 131 mm (96 × 96 DPI)*

hours, respectively. The physical parameters of the unbiased ferrite resonator used in the antenna design are summarised in Table 1. The curves show that the FRA designed with a material processed at 800°C has resonant frequency at 3.8 GHz, while the antenna with ferrite resonator processed at 900°C has resonant frequency at 3.6 GHz, and low return losses. These antennas are suitable to operate in the bands used for 3G WiMAX systems.

For comparison, the simulated and measured insertion losses of the unbiased FRA using a ferrite resonator processed at 900°C are shown in Fig. 8. The measured resonant frequency is 3.61 GHz with an insertion loss $S_{11} = -27.23$ dB, $BW = 248$ MHz. A good agreement is observed between simulation and measurement for both resonant frequency and bandwidth.

Fig. 9 shows 3D simulated radiation pattern and the corresponding directivity values for the FRA processed at 900°C. The antenna shows a directional radiation performance with maximum energy concentration in the broadside direction.

Fig. 10 shows the reflection coefficient frequency behaviour plotted using the Smith chart for the FRA processed at 900°C. At the resonant frequency, the measured input impedance of the ferrite antenna is $45.6 + j1.26$ (Ω). This value was found for the minimum of the return loss at 3.61 GHz (Fig. 8).

Fig. 11 depicts the influence of the applied dc magnetic field on the return loss of the $NiFe_2O_4$ FRA prototype, as function of frequency. Good agreement is observed between these results and the simulated ones presented in Fig. 8.

In addition, we would like to point out that with the knowledge of the applied biasing field, saturation magnetisation of the ferrite, measured magnetic hysteresis curve, and gyromagnetic ratio, we determined the components of the magnetic permeability tensor (μ and k) as function of frequency. The expressions for these components are shown in (1)–(3) and are implemented in the HFSS software.

5 Conclusion

It is pointed out that $NiFe_2O_4$can be used to obtain a homogeneous composite in nanoscale. The hysteresis loops and magnetisation of the ferrimagnetic composite were obtained. The synthesised $NiFe_2O_4$ material properties are suitable for the development of FRA at microwave frequencies.

Numerical results of frequency responses of the proposed FRA were performed using HFSS. The results demonstrate that the FRA antenna exhibits resonant frequency tuning with the application of a magnetic bias field H_0. In addition, the proposed FRA has

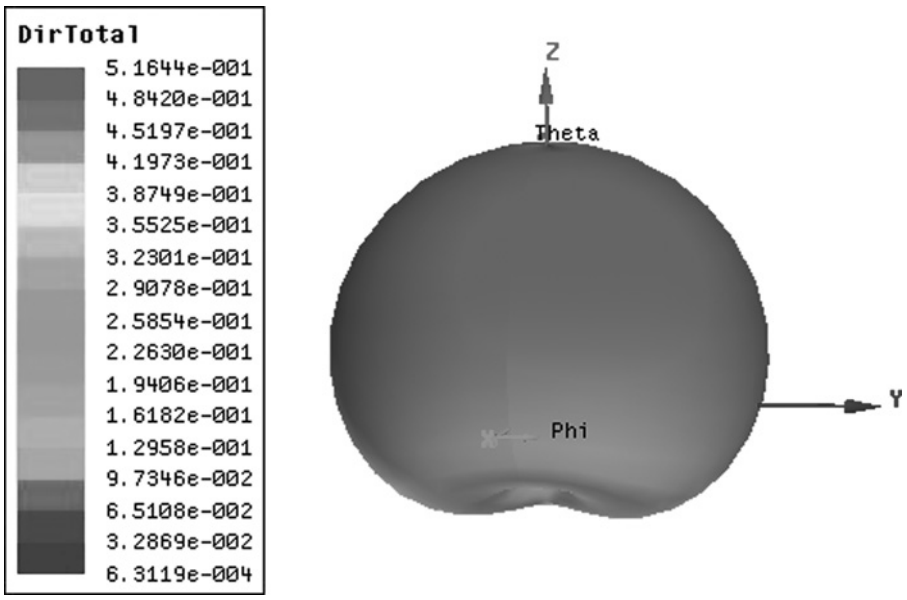

Fig. 9 *Three-dimensional (3D) radiation pattern 125 × 87 mm (96 × 96 DPI)*

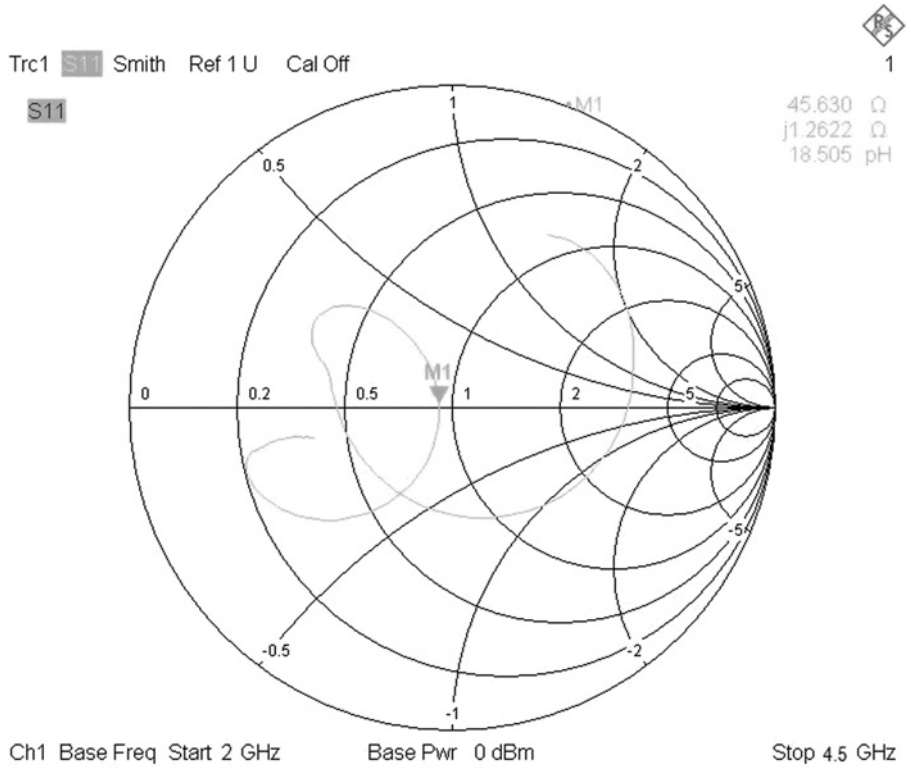

Fig. 10 *Measured input impedance results 183 × 161 mm (96 × 96 DPI)*

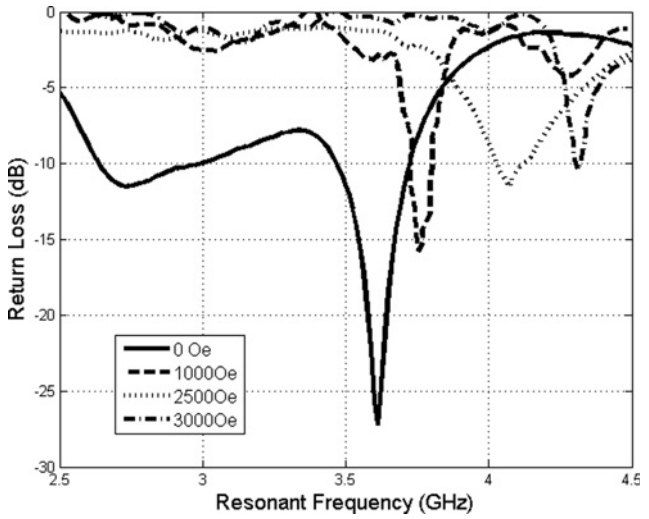

Fig. 11 *Measured return loss results for different values of the magnetic-bias field 174 × 131 mm (96 × 96 DPI)*

reduced dimensions compared to the conventional antenna, allowing miniaturisation, yielding suitable results for microwave applications such as mobile communication and satellite systems. The results demonstrated that the unbiased FRA based on nickel ferrite ($NiFe_2O_4$) can operate for WiMAX applications, in the frequency range around 3.5 GHz, with a relative bandwidth of 12%, approximately. A good agreement between simulation and measurements was observed.

6 Acknowledgment

The authors thank the financial support from the following Brazilian research financing institutions: CNPq/Universal 14/2011 under covenant 481288/2011-2; RECAM under covenant 564913/2010-3; MCT/CNPq under covenant 74/2010; CNPq under covenant 573939/2008-0 (INCT-CSF).

7 References

1 Dong, C., Wang, G., Guo, D., *et al.*: 'Growth, structure, morphology, and magnetic properties of Ni ferrite films', *Nanoscale Res. Lett.*, 2013, **8**, (196), pp. 1–5
2 Kondo, K., Chiba, T., Yamada, S.: 'Effect of microstructure on magnetic properties of Ni–Zn ferrites', *J. Magn. Magnetic Mater.*, 2003, **254–255**, (1), pp. 541–543
3 Rezlescu, N., Iftimie, N., Rezlescu, E., *et al.*: 'Semiconducting gas sensor for acetone based on the fine grained nickel ferrite', *Sens. Actuators B Chem.*, 2006, **114**, (1), pp. 427–432
4 Alcántara, R., Jaraba, M., Lavela, P., *et al.*: 'Changes in oxidation state and magnetic order of iron atoms during the electrochemical reaction of lithium with $NiFe_2O_4$', *Electrochem. Commun.*, 2003, **5**, (1), pp. 16–21
5 Lavela, P., Tirado, J.L.: '$CoFe_2O_4$ and $NiFe_2O_4$ synthesized by sol–gel procedures for their use as anode materials for Li ion batteries', *J. Power Sources*, 2007, **172**, (1), pp. 379–387
6 Borah, K., Bhattacharyya, N.S.: 'Magnetodielectric composite with $NiFe_2O_4$ inclusions as substrates for microstrip antennas', *IEEE Trans. Dielectr. Electr. Insul.*, 2012, **19**, (5), pp. 1825–1832
7 Segal, D.: 'Chemical synthesis of ceramic materials', *J. Mater. Chem.*, 1997, **7**, (8), pp. 1297–1305
8 Oliveira, E.E.C., D'Assunção, A.G., Oliveira, J.B.L., *et al.*: 'Aperture coupled $BaTiO_3$ based dielectric resonator antenna with dual-band', *Microw. Opt. Technol. Lett.*, 2013, **55**, (11), pp. 2759–2763
9 Medeiros, J.L.G., Araújo, W.C., D'Assunção, A.G., *et al.*: 'Investigation on ZPT ceramics applied as dielectric resonator antenna for ultra wideband systems', *Microw. Opt. Technol. Lett.*, 2013, **55**, (6), pp. 1352–1355
10 Petosa, A.: 'Dielectric resonator antenna handbook' (Artech House, 2007)
11 Fechine, P.B.A., Rocha, H.H.B., Moretzsohn, R.S.T., *et al.*: 'Study of a microwave ferrite resonator antenna, based on a ferrimagnetic composite $(Gd_3Fe_5O_{12})$ $GdIG_x$-$(Y_3Fe_5O_{12})YIG_{1-x}$', *IET Microw. Antennas Propag.*, 2009, **3**, (8), pp. 1191–1198
12 Petosa, A., Mongia, R.K., Ittipiboon, A., *et al.*: 'Switchable LP/CP ferrite disk resonator antenna', *Electron. Lett.*, 1995, **31**, (3), pp. 148–149
13 Zervos, T., Alexandridis, A.A., Lazarakis, F., *et al.*: 'Design of a polarisation reconfigurable patch antenna using ferrimagnetic materials', *IET Microw. Antennas Propag.*, 2012, **6**, (2), pp. 158–164
14 Albuquerque, M.R.M.L., Silva, S.G., Oliveira, J.R.S., *et al.*: 'Effect of substrate height variations on radiation properties of microstrip patch antennas on ferrite', *Microw. Opt. Technol. Lett.*, 2005, **44**, (3), pp. 289–292
15 Lax, B., Button, K.J.: 'Microwave ferrites and ferrimagnetics' (McGraw-Hill, 1962)